Organometallics **2001,** *20,* 5067−5075 5067

Structural and Dynamic Features of Bis[2-(2-furyl)indenyl]zirconium Derivatives[†]

Thorsten Dreier, Klaus Bergander, Elina Wegelius,[‡] Roland Fröhlich,[‡] and
Gerhard Erker*

Organisch-Chemisches Institut der Universität Münster, Corrensstrasse 40,
D-48149 Münster, Germany

Received May 29, 2001

Downloaded by CARLI CONSORTIUM on June 29, 2009
Published on October 19, 2001 on http://pubs.acs.org | doi: 10.1021/om0104518

Treatment of 2-indanone with 2-lithio-5-methylfuran, followed by hydrolysis, dehydration, deprotonation with *n*-butyllithium, and transmetalation, gave bis[2-(5-methyl-2-furyl)indenyl]-zirconium dichloride (**6a**). The dynamic 600 MHz ^{1}H NMR spectroscopic analysis in the temperature range between 253 and 128 K revealed the presence of two metallocene conformational isomers in a 60:40 ratio. It is likely that this observed feature just originates from freezing out the indenyl−furyl rotation. The corresponding activation barrier of **6a** was determined at $\Delta G^{\ddagger}_{\mathrm{rot}} = 7.0 \pm 0.4$ kcal mol^{-1} by a line shape analysis. A series of analogous 5-methyl-2-furyl- and 5-methyl-2-thienyl-substituted bis(indenyl)zirconium dibromides and dichlorides show analogous conformational behavior and almost identical rotational activation energies. In the bis[2-(5-methyl-2-furyl)indenyl]ZrR$_2$ series the metallocene rotational barrier can apparently be frozen on the 600 MHz ^{1}H NMR time scale for R = CH$_2$CMe$_3$ and R = CH$_2$Ph. The di(neopentyl)Zr complex **7b** shows a metallocene rotational barrier of $\Delta G^{\ddagger}_{\mathrm{rot(Cp)}}(213\ \mathrm{K}) = 9.0 \pm 0.3$ kcal mol^{-1}, and for the di(benzyl)Zr complex **7c** a $\Delta G^{\ddagger}_{\mathrm{rot(Cp)}}$ value of 11.4 ± 0.3 kcal mol^{-1} was obtained at 243 K. In the cases of **7b** and **7c** only chiral *rac*-type metallocene conformers were found in solution within the limits of the accuracy of the ^{1}H NMR method. The complexes bis[2-(5-ethyl-2-furyl)indenyl]ZrCl$_2$ (**8**) and bis[2-(5-methyl-2-furyl)indenyl]Zr(neopentyl)$_2$ (**7b**) were characterized by X-ray crystal structure analyses. In the solid state both complexes exhibit chiral *rac*-like metallocene frameworks.

Introduction

Bis(2-arylindenyl)zirconium complexes (**1**) were shown to feature two distinctly different conformational isomers in the crystal that can be described as *rac*-**1** and *meso*-**1** metallocene conformers (see Chart 1).[1] Complexes **1** give homogeneous Ziegler−Natta catalysts when activated with methylalumoxane (MAO) that have been used for the formation of high molecular weight polypropylenes that exhibit elastomeric properties. The conformational equilibration of the *rac*- and *meso*-bis(2-arylindenyl)zirconium frameworks during the polymerization process was suggested to be a decisive feature for the production of the elastomeric polyolefins at such catalysts.[1,2]

Unfortunately, the corresponding *meso*-bis(2-arylindenyl)zirconium conformational isomers have not been detected so far to our knowledge in solution, potentially because of an energy difference of ≥1.5 kcal mol^{-1} between the isomers.[3] A variety of examples were investigated by temperature-dependent NMR spectroscopy, but either the conformational equilibration of these systems was too fast to become frozen on the NMR time scale [e.g., (2-arylindenyl)$_2$ZrCl$_2$ systems] or only degenerate enantiomerization of *rac*-conformers was observed [e.g., (2-arylindenyl)$_2$Zr(benzyl)$_2$ examples].[2,3]

We have recently described a series of related (2-hetarylindenyl)$_2$zirconium and -hafnium complexes, such as bis[2-(5-methyl-2-furyl)indenyl]zirconium dichloride (**6a**).[4,6] This shows a *meso*-like structure in the

---

[†] Dedicated to Professor Dieter Hoppe on the occasion of his 60th birthday.

* To whom correspondence should be addressed. Fax: +49 251 8336503. E-mail: erker@uni-muenster.de.

[‡] Performed the X-ray crystal structure analyses.

(1) Waymouth, R. M.; Coates, G. W. *Science* **1995**, *267*, 217−219. Hauptmann, E.; Waymouth, R. M.; Ziller, J. W. *J. Am. Chem. Soc.* **1995**, *117*, 11586−11587.

(2) Collette, J. W.; Tullock, C. W.; MacDonald, R. N.; Buck, W. H.; Su, A. C. L.; Harrell, J. R.; Mülhaupt, R.; Anderson, B. C. *Macromolecules* **1989**, *22*, 3851−3866. Gauthier, W. J.; Collins, S. *Macromolecules* **1995**, *28*, 3779−3786. Pietsch, M. A.; Rappé, A. K. *J. Am. Chem. Soc.* **1996**, *118*, 10908−10909. Bruce, M. D.; Coates, G. W.; Hauptmann, E.; Waymouth, R. M.; Ziller, J. W. *J. Am. Chem. Soc.* **1997**, *119*, 11174−11182. Maciejewski Petoff, J. L.; Bruce, M. D.; Waymouth, R. M.; Masood, A.; Lal, T. K.; Quan, R. W.; Behrend, S. J. *Organometallics* **1997**, *16*, 5909−5916. Kravchenko, R.; Masood, A.; Waymouth, R. M.; Myers, C. L. *J. Am. Chem. Soc.* **1998**, *120*, 2039−2046. Hu, T.; Kreichi, M. T.; Shah, C. D.; Myers, C. L.; Waymouth, R. M. *Macromolecules* **1998**, *31*, 6908−6916. Maciejewski Petoff, J. L.; Agoston, T.; Lal, T. K.; Waymouth, R. M. *J. Am. Chem. Soc.* **1998**, *120*, 11316−11322, and references therein. Tagge, C. D.; Kravchenko, R. L.; Lal, T. K.; Waymouth, R. W. *Organometallics* **1999**, *18*, 380−388. Witte, P.; Lal, T. K.; Waymouth, R. M. *Organometallics* **1999**, *18*, 4147−4155. Maciejewski Petoff, J. L.; Myers, C. L.; Waymouth, R. M. *Macromolecules* **1999**, *32*, 7984−7989. Lin, S.; Waymouth, R. M. *Macromolecules* **1999**, *32*, 8283−8290. Nele, M.; Collins, S.; Dias, M. L.; Pinto, J. C.; Lin, S.; Waymouth, R. M. *Macromolecules* **2000**, *33*, 7249−7260. Lin, S.; Tagge, C. D.; Waymouth, R. M.; Nele, M.; Collins, S.; Pinto, J. C. *J. Am. Chem. Soc.* **2000**, *122*, 11275−11285.

(3) Schneider, N.; Schaper, F.; Schmidt, K.; Kirsten, R.; Geyer, A.; Brintzinger, H. H. *Organometallics* **2000**, *19*, 3597−3604.

(4) Dreier, T.; Erker, G.; Fröhlich, R.; Wibbeling, B. *Organometallics* **2000**, *19*, 4095−4103.

(5) Dreier, T.; Fröhlich, R.; Erker, G. *J. Organomet. Chem.* **2001**, *621*, 197−206.

(6) Ewen, J. A.; Jones, R. L.; Elder, M. J.; Rheingold, A. L.; Liable-Sands, L. M. *J. Am. Chem. Soc.* **1998**, *120*, 10786−10787.

10.1021/om0104518 CCC: $20.00 © 2001 American Chemical Society
Publication on Web 10/19/2001

Downloaded by CARLI CONSORTIUM on June 29, 2009
Published on October 19, 2001 on http://pubs.acs.org | doi: 10.1021/om0104518

Chart 1. Structurally Characterized Bis(2-aryl)- and Bis(2-hetaryl)indenylzirconium Complexes

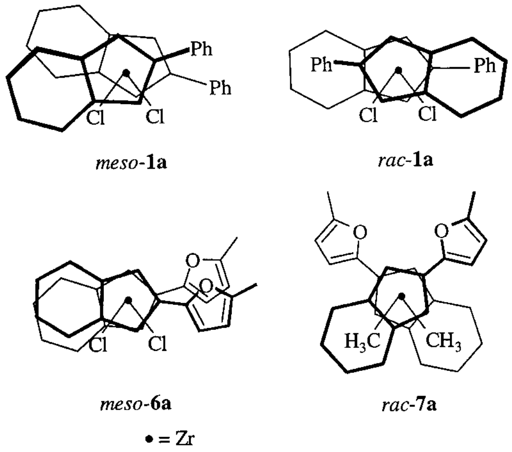

meso-**1a** *rac*-**1a** *meso*-**6a** *rac*-**7a**

• = Zr

crystal, whereas its bis[2-(5-methyl-2-furyl)indenyl]zirconium dimethyl derivative (**7a**) exhibits a *rac*-structure in the solid state (see Chart 1). These furyl-substituted systems also generate efficient Ziegler–Natta catalysts for elastomeric polypropylene formation upon treatment with MAO. We have now investigated the conformational features of a variety of substituted bis[2-(5-alkyl-2-furyl)]- and bis[2-(5-alkyl-2-thienyl)indenyl]zirconium systems by dynamic NMR spectroscopy and found that here some dynamic features even at the stage of the metallocene dihalides could be frozen out on the NMR time scale under certain experimental conditions.[7]

Results and Discussion

Bis[2-(5-alkyl-2-furyl)indenyl]zirconium Dihalides. The synthesis and X-ray crystal structure analysis of bis[2-(5-methyl-2-furyl)]zirconium dichloride (**6a**) was recently described by us.[4] The synthesis starts by the addition of 2-lithio-5-methylfuran to 2-indanone.[8] Deprotonation of the resulting 2-(5-methyl-2-furyl)-indene with *n*-butyllithium followed by treatment with zirconium tetrachloride gave **6a**. Complex **6a** exhibits temperature-dependent dynamic ^{1}H NMR spectra (600 MHz) which could be brought to a static low-temperature limiting situation by using a mixture of $CDFCl_2$ and CDF_2Cl as the solvent[9] (see Figure 1).

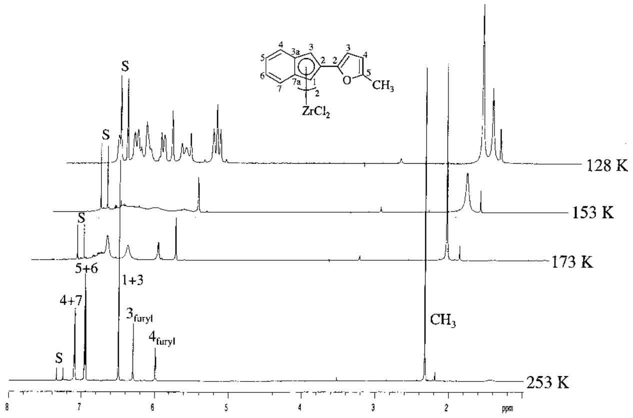

Figure 1. Dynamic ^{1}H NMR spectra (600 MHz) of complex **6a** in $CDFCl_2$/CDF_2Cl.

Scheme 1

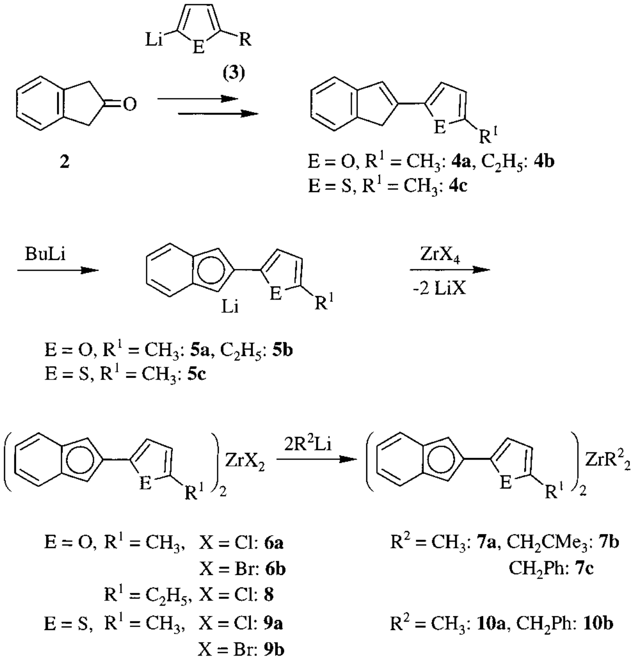

In such a situation the potential formation of a total of six conformational diastereomers must be considered. They shall be tagged by the letters **A** to **F** as depicted in Scheme 2. There are three isomers (**A**, **B**, **E**) with *rac*-like metallocene frameworks and three (**C**, **D**, **F**) with *meso*-like skeletons. The latter will under experimental conditions probably exhibit averaged C_s-symmetric core-frameworks; the *rac*-like isomers must be considered to exhibit chiral C_2-symmetric cores under the experimental conditions.[10] Thus, the three isomers of each of the sets to a first approximation are distinguished by their relative orientations of the 5-methyl-2-furyl substituents at their perimeter. As we have seen from the many known structures, the furyl substituents are arranged coplanar with the indenyl planes. At the bent metallocene framework the furyl groups can then be arranged with their oxygen atoms pointing toward the front side or toward the narrow back side of the bent metallocene wedge. Thus a simple metallocene rotation interconverts, for example, the *rac*-front-side isomer **A** (i.e., the isomer that exhibits the furyl oxygen atoms both oriented toward the open front side of the bent metallocene wedge) with the *rac*-back-side isomer **B** and so forth.

At 253 K a simple ^{1}H NMR spectrum of complex **6a** is monitored featuring a single sharp methyl resonance at δ 2.48, the furyl 3-H and 4-H signals at δ 6.64 and 6.14, the indenyl 1-H/3-H resonance at δ 6.64, and the indenyl arene 4-H/7-H and 5-H/6-H resonances at δ 7.24 and 7.10, respectively. The latter two signals have broadened considerably at 173 K and have almost disappeared in the baseline at 153 K. At this temperature, the furyl 3-H signal has also become very broad

---

(7) For a related study see: Erker, G.; Aulbach, M.; Knickmeier, M.; Wingbermühle, D.; Krüger, C.; Nolte, M.; Werner, S. *J. Am. Chem. Soc.* **1993**, *115*, 4590–4601. Knickmeier, M.; Erker, G.; Fox, T. *J. Am. Chem. Soc.* **1996**, *118*, 9623–9630.

(8) Paquette, L. A.; Bauer, W.; Sivik, M. R.; Bühl, M.; Feigel, M.; Schleyer, P. v. R. *J. Am. Chem. Soc.* **1990**, *112*, 8776–8789.

(9) Siegel, J. S.; Anet, F. A. *J. Org. Chem.* **1988**, *53*, 2629–2630.

(10) Piemontesi, F.; Camurati, I.; Resconi, L.; Balboni, D.; Sironi, A.; Moret, M.; Zeigler, R.; Piccolrovazzi, N. *Organometallics* **1995**, *14*, 1256–1266. We thank a careful reviewer for several interesting and helpful suggestions.

Downloaded by CARLI CONSORTIUM on June 29, 2009
Published on October 19, 2001 on http://pubs.acs.org | doi: 10.1021/om0104518

Scheme 2. Schematic Representation of Possible Rotameric Isomer Structures of 6a

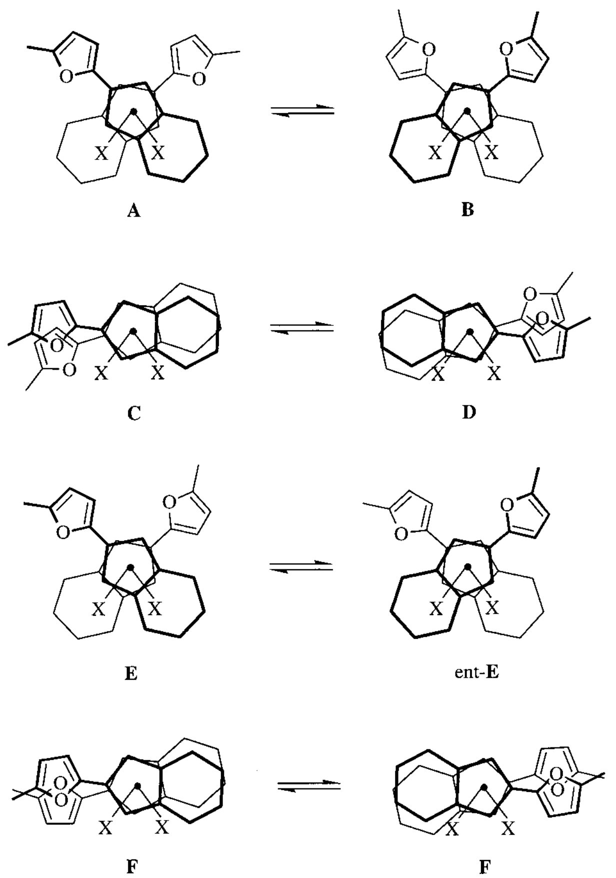

and the furyl-methyl resonance shows considerable broadening (see Figure 1). At 128 K decoalescence is achieved. We observe an overlapping pattern of at least 14 resonances in the aromatic region (potentially corresponding to a total of 16 different protons) and a pair of methyl resonances at δ 2.57 and 2.44 in a 60:40 ratio. Since the methyl resonances are not found in an equimolar ratio, we must conclude that two diastereomeric metallocene conformers are present in solution and detected in the static ^{1}H NMR spectrum at 128 K (600 MHz) under these conditions. From the observed behavior in the temperature range 173−153 K (and additional evidence from other related molecules that will be presented below) it is possible that in complex **6a** the metallocene rotation is frozen out, coinciding with or very narrowly followed by freezing the rotation around the indenyl C2-furyl C2 vector. From a line shape analysis[11] of the furyl-CH$_3$ ^{1}H NMR resonances a Gibbs activation energy of $\Delta G^{\ddagger}_{\mathrm{rot(Cp)}} \approx \Delta G^{\ddagger}_{\mathrm{rot(Ar)}} = 7.0 \pm 0.3$ kcal mol^{-1} was calculated for the **6a** (major) to **6a** (minor) conformational equilibration. Alternatively, this spectroscopic behavior could indicate that the metal−indenyl rotation is still rapid at 128 K and that we are freezing out the Cp−furyl rotation under our experimental conditions. This would lead to the observation of two sets of ^{1}H NMR spectra originating from an (averaged) chiral C_2-symmetric and achiral C_s-symmetric arrangement of the planarly chiral furyl substituents that are arranged coplanar with their adjacent Cp rings. The observed Gibbs activation energy would then correspond to $\Delta G^{\ddagger}_{\mathrm{rot(Ar)}}$. In view of the behavior of the related complexes **7b**, **7c**, and **10b** (see below), this is an attractive interpretation.

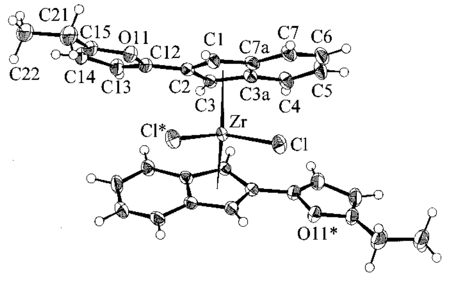

Figure 2. View of the molecular structure of complex **8** in the crystal, featuring a chiral (*rac*) metallocene conformation. Selected bond lengths (Å), angles, and dihedral angles (deg): Zr−C1 2.557(2), Zr−C2 2.548(2), Zr−C3 2.454(2), Zr−C3a 2.523(2), Zr−C7a 2.607(2), Zr−C_{Cp} 2.323, Zr−Cl 2.4175(5), C1−C2 1.412(2), C1−C7a 1.417(2), C2−C3 1.416(2), C2−C12 1.445(2), C3−C3a 1.431(2), C3a−C7a 1.424(2), C3a−C4 1.416(2), C4−C5 1.363(3), C5−C6 1.406(3), C6−C7 1.357(3), C7−C7a 1.416(2), O11−C12 1.369(2), O11−C15 1.371(2), C12−C13 1.344(3), C13−C14 1.427(3), C14−C15 1.334(2), C15−C21 1.481(3), C21−C22 1.512(3); C_{Cp}−Zr−C_{Cp}* 132.8, Cl−Zr−Cl* 97.44(3), C1−C2−C3 108.5(2), C1−C2−C12 125.2(2), C12−C2−C3 126.3(2), C2−C3−C3a 107.4(2), C3−C3a−C7a 107.8(1), C3−C3a−C4 132.8(2), C3a−C7a−C7 120.3(2), C3a−C7a−C1 107.8(2), C2−C12−O11 115.4(2), C12−O11−C15 106.9(3).

Bis[2-(5-ethyl-2-furyl)indenyl]ZrCl$_2$ (**8**) was studied as a second substituted furylindenyl zirconium dichloride complex example in solution. In this case the topological NMR situation is more complex: in all the systems **6**−**10** shown in Scheme 1 freezing of either the metal−Cp rotation or the rotation about the Cp−furyl vector (or both, of course) in the complex will result in diastereotopic splitting of the −CH$_2$− hydrogen atoms of the furyl-attached ethyl groups. But aside from this spectral complication a conformational behavior similar to that observed in complex **6a** is expected.

The synthesis of bis[2-(5-ethyl-2-furyl)indenyl]ZrCl$_2$ (**8**) was carried out as outlined in Scheme 1. 2-Ethylfuran was deprotonated by treatment with *n*-butyllithium. The resulting 2-lithio-5-ethylfuran reagent (**3b**) was added to 2-indanone, hydrolyzed, and dehydrated to yield **4b**. Subsequent deprotonation by treatment with n-BuLi followed by transmetalation gave complex **8** (35% isolated after crystallization from toluene at −30 °C). The obtained crystals were suitable for an X-ray crystal structure analysis of **8**. In the crystal complex **8** exhibits a single C_2-symmetric rotational isomer. The conformation of **8** in the solid state represents an example of the *rac*-conformer type **A** (see Scheme 2). The two symmetry-equivalent furyl substituents are oriented coplanar with the indenyl ligand frameworks. Their oxygen atoms point toward the open front side of the bent metallocene wedge. Even the carbon atoms of the furyl substituents are arranged in the overall ligand plane (see Figure 2). The bonding features of the metallocene core are in a typical range (Cl1−Zr 2.417(5), Cl1−Zr−Cl1* 97.44(3)°, Cp(centroid)−Zr−Cp(centroid) angle 132.8°).

In CDFCl$_2$/CDF$_2$Cl solution complex **8** shows a temperature-dependent ^{1}H NMR behavior analogous to that

---

[11] Kleier, D. A.; Binsch, G. *DNMR 3*; Indiana University, 1970. Kleier, D. A.; Binsch, D. *J. Magn. Reson.* **1970**, *3*, 146−160. Marat, K. *XSIM*; University of Manitoba, 1997. Green, M. L. H.; Wong, L.-L.; Seela, A. *Organometallics* **1992**, *11*, 2660−2668, and references therein.

Downloaded by CARLI CONSORTIUM on June 29, 2009
Published on October 19, 2001 on http://pubs.acs.org | doi: 10.1021/om0104518

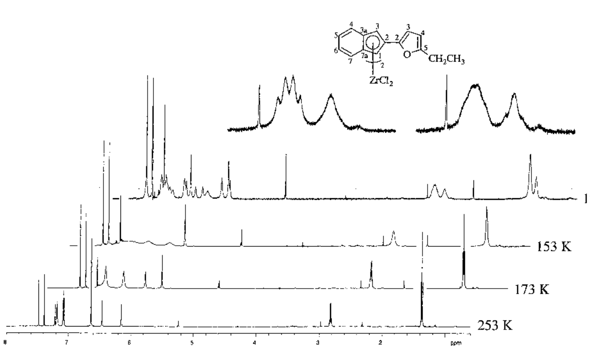

Figure 3. Dynamic ^{1}H NMR spectra of complex **8**. The insets show the appearance of the signals of the diastereomeric methylene protons of the two diastereomers upon decoupling by irradiation at their respective CH$_3$ resonances.

previously observed for **6a** (see above). At 253 K it shows a single set of three ^{1}H NMR signals originating from the indenyl framework, two signals of the furyl protons, and the quartet/triplet features of the furyl-CH$_2$CH$_3$ substituent (see Figure 3). All these signals rapidly get broad upon lowering the temperature and decoalesce to two sets of ligand signals in a ca. 65:35 ratio. The ^{1}H NMR spectrum at 128 K under static conditions shows two broadened methyl signals at δ 1.37 and 1.27 and two broad $-$CH$_2-$ multiplets at δ 2.88 and 2.73. The methylene signals are both too broad to allow for the required analysis of the spin pattern under static ^{1}H NMR conditions. Therefore, we have performed two decoupling experiments (see insets in Figure 3). Irradiation at the position of the methyl group of the major isomer (δ 1.37) resulted in the observation of an AB quartet of the adjacent methylene group, centered at δ 2.86 (δ^A = 2.88, δ^B = 2.84, $^2J_{AB} \approx$ 16 Hz). This experiment left the appearance of the CH$_2$ signal of the minor isomer unchanged, of course. However, irradiation at the position of the CH$_3$ resonance of the minor isomer (δ 1.27) resulted in the observation of a narrow AB quartet (δ^A = 2.70, δ^B = 2.68, $^2J_{AB} \approx$ 16 Hz) of its attached $-$CH$_2-$ group (see Figure 3). Thus, both observed conformers of complex **8** exhibit diastereotopic $-$CH^{A}H$^B-$ moieties under static ^{1}H NMR conditions at low temperature, as expected. Again, it cannot be decided which pair of *rac*- or *meso*-conformers from the **A** to **F** set (see Scheme 2) is present in solution.

Line shape analysis[11] gave an observed activation barrier of $\Delta G^{\ddagger}_{rot}$ = 7.1 ± 0.4 kcal mol^{-1} for the conformational equilibration of **8**. Again, it is likely that only the indenyl$-$furyl rotation became frozen on the ^{1}H NMR time scale under these conditions.

We have also investigated the temperature-dependent dynamic ^{1}H NMR of bis[2-(5-methyl-2-furyl)indenyl]-ZrBr$_2$ (**6b**) and the corresponding bis[2-(5-methyl-2-thienyl)indenyl]ZrX$_2$ complexes **9a** (X = Cl) and **9b** (X = Br). They all showed an analogous conformational behavior, each exhibiting the spectra of a diastereomeric pair of rotational isomers below the coalescence temperature. The activation energies $\Delta G^{\ddagger}_{rot}$ in these cases were all very similar (ca. 7 kcal mol^{-1}; see Table 1).

Table 1. Activation Energies ($\Delta G^{\ddagger}_{rot}$) of the Observed Conformational Equilibration of the Bis[2-(5-alkyl-2-hetaryl)indenyl]ZrX$_2$ Complexes 6, 8, and 9 as Determined from Their Dynamic ^{1}H NMR Spectra (600 MHz, in CDFCl$_2$/CDF$_2$Cl) by Line Shape Analysis.

compd	X	subst	*T* (K)	δ_{CH_3}[b]	ratio	ΔG_{rot}[a]
6a	Cl	Me-furyl	143	2.41, 2.28	60:40	7.0
6b	Br	Me-furyl	143	2.58, 2.42[c]	70:30	7.2
8	Cl	Et-furyl	143	1.37, 1.27	60:40	7.1
9a	Cl	Me-thienyl	133	2.60, 2.57	44:56	6.7
9b	Br	Me-thienyl	138	2.59, 2.56	50:50	6.9

[a] ±0.4 kcal mol^{-1}. [b] At 133 K. [c] At 128 K.

Behavior of the Corresponding Bis[2-(5-alkyl-2-furyl)indenyl]zirconium Dialkyl Complexes. The catalytic polypropylene elastomer formation at the bis(2-hetarylindenyl) group 4 metal complexes requires the presence of active Zr$-$C σ-bonds.[12] Therefore, we included investigation of the conformational behavior of several examples of the respective dialkylmetallocene systems in this study.

Dimethylbis[2-(5-methyl-2-furyl)indenyl]zirconium (**7a**) was prepared by treatment of **6a** with 2 molar equiv of methyllithium, as recently described by us. The presence of the two σ-methyl ligands resulted in a marked change of the dynamic behavior of the complex. The system remained dynamic down to the lowest possible temperature (128 K) in the CDFCl$_2$/CDF$_2$Cl Freon solvent mixture.

Attaching bulky σ-neopentyl or σ-benzyl ligands at zirconium has an opposite effect in these systems.[2,3] The bis[2-(5-methyl-2-furyl)indenyl]di(neopentyl)zirconium complex **7b** was prepared by treatment of the metallocene dichloride **6a** with 2 equiv of neopentyllithium. Complex **7b** was isolated in 60% yield after crystallization from pentane. Single crystals obtained from pentane were suitable for an X-ray crystal structure analysis. Complex **7b** also exhibits a chiral C_2-symmetric metallocene conformation in the solid state. The observed specific rotamer represents an example of the *rac*-type **A** conformer (as depicted in Scheme 2). The furyl groups are arranged coplanar with the η^5-indenyl planes, and they have their oxygen atoms oriented toward the front sector of the bent metallocene wedge. The σ-neopentyl ligands are arranged C_2-symmetrically at the front of the bent metallocene. Their bulky *tert*-butyl groups are pointing away from the core of the metallocene (dihedral angles C31*$-$Zr$-$C31$-$C32 $-$66.7(7)°, Cp(centroid)$-$Zr$-$C31$-$C32 $-$178.5°, Cp*(centroid)$-$Zr$-$C31$-$C32 42.3°). The Zr$-$C(31) bond length is 2.256(3) Å, and the C31*$-$Zr$-$C31 angle of the σ-ligands at zirconium amounts to 100.7(3)°.

The attachment of $-$CH$_2-$R groups in the σ-ligand plane of the bent metallocene unit has also resulted in the introduction of a chirality sensor into the molecule. Under static conditions a C_2-symmetric metallocene framework would render the pair of $-$CH$_2$R σ-substituents homotopic, but the pairs of the $-$CH$_2-$ hydrogens at each individual $-$CH$_2-$R group would be diastereotopic. In contrast, the two $-$CH$_2$R groups at a substituted C_s-symmetric (*meso*) bis(indenyl)zirconium framework would be expected to be diastereotopic, but with the $-$CH$_2-$ hydrogens of each individual $-$CH$_2$R σ-ligand being enantiotopic.

---

(12) Brintzinger, H.-H.; Fischer, D.; Mülhaupt, R.; Rieger, B.; Waymouth, R. M. *Angew. Chem.* **1995**, *107*, 1255$-$1283; *Angew. Chem., Int. Ed. Engl.* **1995**, *34*, 1143$-$1170, and references therein.

Downloaded by CARLI CONSORTIUM on June 29, 2009
Published on October 19, 2001 on http://pubs.acs.org | doi: 10.1021/om0104518

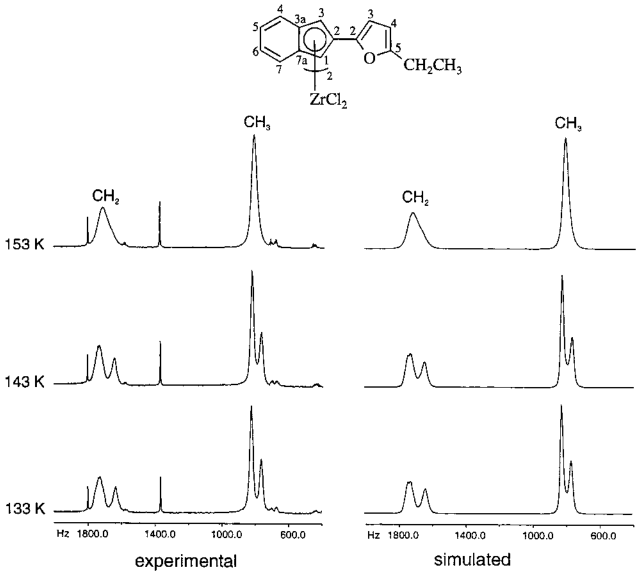

Figure 4. Experimental (600 MHz in $CDFCl_2/CDF_2Cl$) and calculated ^1H NMR spectra arising from the conformational equilibration of **8** (only the signals of the (furyl)-CH_2CH_3 groups are depicted).

Scheme 3

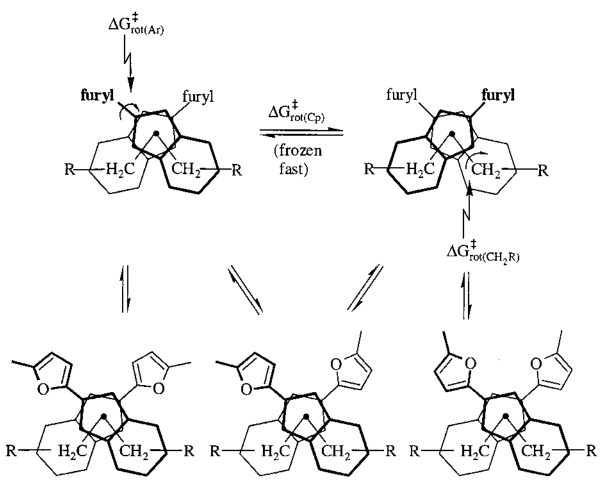

In reality, the dynamic features of complex **7b** are determined by the magnitude of three activation barriers of conformational equilibration, namely, $\Delta G^{\ddagger}_{rot(Cp)}$, the barrier of rotation about the metal–η^5-indenyl vector, $\Delta G^{\ddagger}_{rot(Ar)}$, the barrier of rotation around the connecting indenyl–furyl σ-bond, and $\Delta G^{\ddagger}_{rot(CH_2R)}$, the rotational barrier of the Zr–C σ-bond (see Scheme 3). From the conformational NMR we assume that the latter, $\Delta G_{rot(CH_2R)}$, probably represents the lowest barrier. It seems that freezing of the Zr–CH_2R rotation was not achieved in any of our experiments, even at the lowest temperature reached (128 K) in the $CDFCl_2/CDF_2Cl$ Freon solvent. Rapid rotation around the Zr–CH_2R σ-bond, and thus rapid equilibration of the possible σ-bond conformers in the whole temperature range, will be assumed for our interpretation.

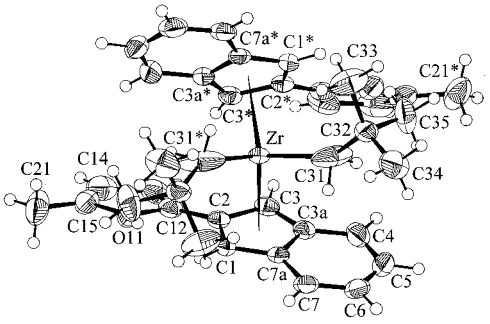

Figure 5. Molecular structure of complex **7b**. Selected bond lengths (Å) and angles (deg): Zr–C1 2.588(2), Zr–C2 2.556(2), Zr–C3 2.520(2), Zr–C3a 2.647(2), Zr–C7a 2.678(2), Zr–C_{Cp} 2.301, Zr–C31 2.256(3), C1–C2 1.412(3), C1–C7a 1.419(3), C2–C3 1.422(3), C2–C12 1.444(4), C3–C3a 1.414(4), C3a–C7a 1.432(4), C3a–C4 1.428(4), C4–C5 1.364(5), C5–C6 1.409(5), C6–C7 1.358(4), C7–C7a 1.417(4), O11–C12 1.370(3), O11–C15 1.379(4), C12–C13 1.352(4), C13–C14 1.419(5), C14–C15 1.334(5), C15–C21 1.489(5); C_{Cp}–Zr–C_{Cp}* 128.5, C31–Zr–C31* 100.7(3), C1–C2–C3 108.3(2), C1–C2–C12 125.4(2), C12–C2–C3 126.4(2), C2–C3–C3a 107.9(2), C3–C3a–C7a 107.8(2), C3–C3a–C4 133.1(3), C3a–C7a–C7 120.0(2), C3a–C7a–C1 107.8(2), C2–C12–O11 116.1(2), C12–O11–C15 106.5(3).

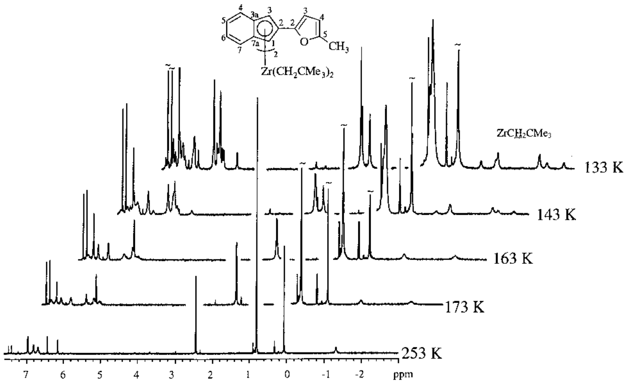

Figure 6. Dynamic ^1H NMR spectra of **7b** (600 MHz, $CDFCl_2/CDF_2Cl$).

The 600 MHz ^1H NMR spectrum of complex **7b** at 253 K is very simple due to rapid equilibration of all conformational processes. It shows three signals of the indenyl hydrogens, two furyl-H resonances (see Figure 6), and a furyl-methyl group singlet. The pair of σ-neopentyl ligands shows a $-C(CH_3)_3$ singlet at δ 0.80 and a broad [Zr]–CH_2– singlet at δ −1.33.

Lowering the temperature first results in a broadening of the three indenyl signals and eventually to their decoalescence to give a total of six individual indenyl-H resonances. At the same time the high-field [Zr]–CH_2– singlet splits into a (broadened) AX spin pair at δ −0.85 and −2.16. This behavior indicates freezing of the Zr–indenyl rotation on the NMR time scale. The diastereotopic splitting of the $-CH_2-$ hydrogens of the $-CH_2-R$ “chirality sensor” indicates that complex **7b** in solution favors a chiral metallocene backbone conformation. At 173 K the metallocene rotation of **7b** has become frozen, but the indenyl–furyl σ-rotation is still rapid under these conditions. From the dynamic NMR spectra of the 253 K to 173 K transition a Gibbs activation barrier of the metallocene rotation was determined at $\Delta G^{\ddagger}_{rot(Cp)} = 9.0 \pm 0.3$ kcal mol^{-1}.[13]

---

[13] Alternatively, this dynamic ^1H NMR spectroscopic behavior could be formally rationalized if rapid metal–indenyl rotation and freezing out of the Zr–CH_2R σ-ligand rotation would be assumed. We regard this possible interpretation less likely in view of the observed values of the activation energies.

Downloaded by CARLI CONSORTIUM on June 29, 2009
Published on October 19, 2001 on http://pubs.acs.org | doi: 10.1021/om0104518

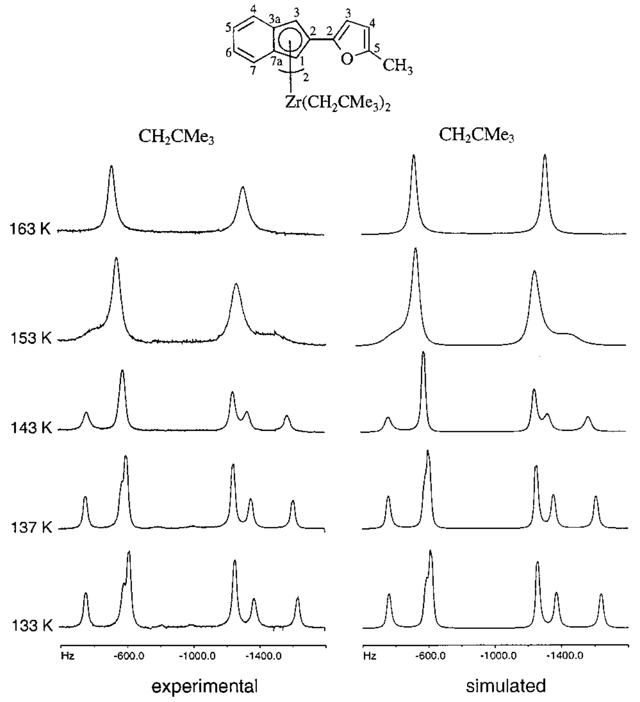

Figure 7. Experimental and calculated 600 MHz ^{1}H NMR spectra of the assumed **7b-A** ⇌ **7b-E** rotational interconversion (only the CH_2CMe$_3$ resonances are depicted).

Further lowering the temperature eventually results in a broadening of the indenyl signals again and further splitting, and decoalescence of the furyl signals (both actually too much overlapping as to allow for a detailed analysis). Also broadening and decoalescence of the furyl−CH$_3$ and further splitting of the [Zr]−CH$_2$−R resonances is observed; all spectral changes now indicate the freezing of the indenyl−furyl σ-rotation. The observed splitting of the [Zr]−CH$_2$−R signals (see Figure 6) indicates the occurrence of two rotameric isomers in solution: one is C_2-symmetric; it is characterized by the appearance of a (broadened) AX system at δ −1.05 and −2.11. This would be in accord with either the conformer **7b-A** or **7b-B** (see Scheme 3). In view of the results of the X-ray crystal structure analysis (see Figure 5) we tentatively assign to it the structure of **7b-A**. The other isomer is of lower symmetry (C_1), as it has both −CH$_2$−R groups differentiated and each split into a (broadened) AX system. This would be consistent with the rotameric structure of **7b-E** to be assigned to this isomer (see Scheme 3). Consequently this rotamer exhibits a pair of furyl−CH$_3$ resonances, whereas the other isomer (**7b-A**) shows only a single furyl−CH$_3$ signal. The two rotamers are found in a ca. 1:1 ratio in this solvent at 133 K. From a line shape analysis the $\Delta G^{\ddagger}_{\mathrm{rot(Ar)}} = 7.1 \pm 0.4$ kcal mol^{-1} value was obtained for the activation energy of the indenyl furyl σ-rotation in complex **7b**, which is in the expected range for this process.

The complex dibenzylbis[2-(5-methylfuryl)indenyl]zirconium (**7c**), prepared by the reaction of **6a** with benzylmagnesium chloride, shows an analogous dynamic behavior (see Figure 8). Freezing of the metallocene rotation seems to have an even higher barrier (**7c**: $\Delta G^{\ddagger}_{\mathrm{rot(Cp)}} = 11.4 \pm 0.3$ kcal mol^{-1}) than **7b**. It results in a splitting of the single −CH_2Ph 600 MHz ^{1}H NMR resonance into a cleanly resolved AX system at 213 K (see Figure 8) followed by a further splitting of these signals into one broadened AX system of the C_2-symmetric **7c-A** rotamer and a pair of AX systems of the **7c-E** isomer (one of these shows a fortuitous double isochrony with one of the **7c-A** resonances). The **7c** $\Delta G^{\ddagger}_{\mathrm{rot(Ar)}} = 7.3 \pm 0.4$ kcal mol^{-1} value, obtained from the line shape analysis, is in the expected range.

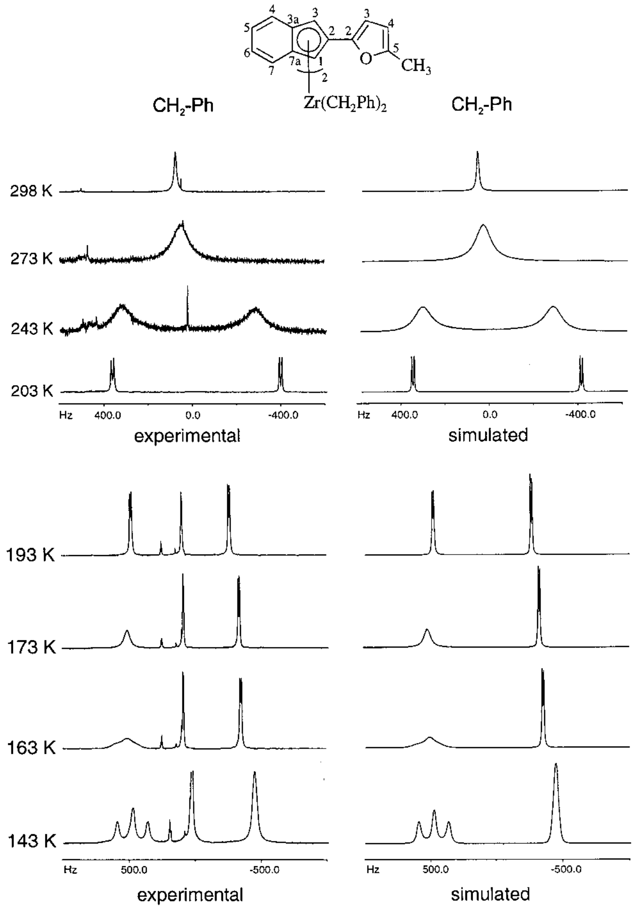

Figure 8. Experimental and calculated dynamic 600 MHz ^{1}H NMR spectra (CH_2Ph resonances) of **7c** illustrating the freezing of the metallocene rotation ($\Delta G^{\ddagger}_{\mathrm{rot(Cp)}} = 11.4 \pm 0.3$ kcal mol^{-1}, in CD$_2$Cl$_2$, top), followed by freezing of the indenyl−furyl σ-bond rotation ($\Delta G^{\ddagger}_{\mathrm{rot(Ar)}} = 7.3 \pm 0.4$ kcal mol^{-1}, in CDFCl$_2$/CDF$_2$Cl, bottom)

Table 2. Activation Energies of [Zr]−(η^5-indenyl) Rotation [$\Delta G^{\ddagger}_{\mathrm{rot(Cp)}}$] and Indenyl−Hetaryl σ-Bond Rotation [$\Delta G^{\ddagger}_{\mathrm{rot(Ar)}}$] of the Complexes 7 and 10[a]

compd	hetaryl	σ-ligand	$\Delta G^{\ddagger}_{\mathrm{rot(Cp)}}$ $(T)^b$	$\Delta G^{\ddagger}_{\mathrm{rot(Ar)}}$ $(T)^c$	[**A**]:[**E**]
7b	Me-furyl	−CH$_2$−CMe$_3$	9.0 (213)	7.1 (143)	50:50
7c	Me-furyl	−CH$_2$−Ph	11.4 (243)	7.3 (163)	45:55
10b	Me-thienyl	−CH$_2$−Ph	12.0 (253)	*d*	*d*

[a] For structures see Scheme 1; $\Delta G^{\ddagger}$ values determined from the dynamic 600 MHz ^{1}H NMR spectra (in CDFCl$_2$/CDF$_2$Cl) by line shape analysis. [b] ±0.3 kcal mol^{-1}. [c] ±0.4 kcal mol^{-1}, temp in K. [d] Not determined.

Dibenzylbis[2-(5-methyl-2-thienyl)indenyl]zirconium (**10b**) shows the same behavior. Here we have followed the slowing of the metallocene rotational process and determined its activation barrier (see Table 2). Dimethylbis[2-(5-methyl-2-thienyl)indenyl]zirconium (**10a**) again is characterized by a much lower barrier of the Zr−indenyl rotation, which could not be frozen out on the

Downloaded by CARLI CONSORTIUM on June 29, 2009
Published on October 19, 2001 on http://pubs.acs.org | doi: 10.1021/om0104518

^{1}H NMR 600 MHz time scale in the temperature range investigated in this study.

Conclusions

Our study has shown that the systems **6**, **7a**, **8**, **9**, and **10a**, which all have rather small σ-ligands of a high local symmetry bonded to the zirconium center, exhibit much lower conformational barriers than the systems **7b**,**c** and **10b**, which contain considerably more bulky σ-neopentyl or σ-benzyl ligands. In the former case it is likely that only the indenyl−furyl (or thienyl) rotation was frozen out on the ^{1}H NMR time scale at very low temperature and that the metal−indenyl rotation was still rapid even at 128 K in the Freon solvent.

In the systems **7b**, **7c**, and **10b** we have probably achieved a successive freezing of the metal−indenyl rotation (i.e., the actual metallocene conformational equilibration) followed by slowing the indenyl−furyl rotation on the ^{1}H NMR time scale. In the furyl systems **7b** and **7c** two conformational isomers were eventually observed that both exhibit the characteristics expected for the bent metallocenes containing chiral *rac*-type frameworks. In no case could we secure the presence of a *meso*-type conformer of these metallocene systems in solution within the limits of the accuracy of the ^{1}H NMR method, although in a few instances such rotational isomers had previously been observed by X-ray diffraction in the solid state.[1,2,4] This further indicates that the *meso*-like conformers of the 2-(het)aryl-substituted bis(indenyl)MR$_2$ systems indeed must be regarded as being markedly higher in energy as opposed to their (ubiquitous) *rac*-like conformational isomers,[3] at least in solution. Whether this extends from the neutral metallocene catalyst precursors to the cationic metallocene Ziegler−Natta catalysts[16,17] that are actually actively involved in the reported elastomeric polypropylene formation[18] must remain an experimentally open question at present, but we must conclude that the actual involvement of a *meso*-metallocene conformer that is undergoing the proposed conformational "switching" process in elastomeric polypropylene formation remains an unproven postulate,[1] until a first example of a 2-substituted *meso*-bis(indenyl) ZrX$_2$ metallocene rotamer has been found in solution and its equilibration with the apparently ubiquitous *rac*-rotational conformer has been demonstrated.

Experimental Section

Reactions were carried out under an argon atmosphere using Schlenk-type glassware or in a glovebox. Solvents (including the deuterated solvents used for NMR spectroscopy) were dried and distilled under argon prior to use. NMR spectra were recorded on a Bruker AC 200 P NMR spectrometer (^{1}H: 200 MHz, ^{13}C: 50 MHz) at 300 K or a Varian Unity Plus NMR spectrometer (^{1}H: 600 MHz, ^{13}C: 150 MHz) at 298 K. 2-(5-Methyl-2-furyl)indenyllithium (**5a**),[4] 2-(5-methyl-2-thienyl)indenyllithium (**5c**),[4] neopentyllithium,[19] bis[2-(5-methyl-2-furyl)indenyl]zirconium dichloride (**6a**),[4] and bis[2-(5-methyl-2-thienyl)indenyl]zirconium dichloride (**9a**)[4] were prepared according to literature procedures. Most of the compounds were characterized by additional GCOSY, GHSQC, and GHMBC NMR experiments;[20] for details see the Supporting Information.

2-(5-Ethyl-2-furyl)indene (4b). A solution of 2-ethylfuran (3.96 g, 41.2 mmol) in diethyl ether (100 mL) was reacted at room temperature with *n*-butyllithium (26.0 mL, 41.6 mmol, 1.60 M in *n*-hexane). After stirring overnight the reaction mixture was cooled to −78 °C and solid 2-indanone (5.44 g, 41.2 mmol) was added by 0.50 g portions over a period of 4 h. The solution was allowed to warm to −25 °C after stirring for an additional 2 h and then hydrolyzed with 2 N HCl (75 mL). After separation of the layers, drying over MgSO$_4$, and column chromatography (isohexane:diethyl ether, 4:1) 4.29 g (20.4 mmol, 50%) of the white product was obtained. Mp: 50 °C. Anal. Calcd for C$_{15}$H$_{14}$O (210.3): C, 85.68; H, 6.71. Found: C, 85.37; H, 7.10. IR (KBr): $\tilde{\nu}$ 3127 (w), 3061 (w), 3044 (w), 2968 (m), 2940 (w), 1690 (w), 1613 (vs), 1575 (s), 1514 (s), 1465 (s), 1394 (m), 1372 (m), 1218 (m), 1010 (vs), 916 (s), 801 (vs), 763 (vs), 719 (vs) cm^{-1}. ^{1}H NMR (dichloromethane-d_2): δ 7.42 (ddd, 1H, 7-H, ^3J = 7.8 Hz, ^4J = 1.2 Hz, ^5J = 0.6 Hz), 7.35 (d, 1H, 4-H, ^3J = 7.2 Hz), 7.25 (dt, 1H, 5-H, ^3J = 7.8 Hz, ^3J = 7.2 Hz, ^4J = 1.2 Hz), 7.15 (dt, 1H, 6-H, ^3J = 7.8 Hz, ^3J = 7.2 Hz, ^4J = 1.2 Hz), 7.00 (s, 1H, 3-H), 6.40 (d, 1H, 3-H$_{\text{furyl}}$, ^3J = 3.0 Hz), 6.08 (dt, 1H, 4-H$_{\text{furyl}}$, ^3J = 3.0 Hz, ^4J = 1.2 Hz), 3.70 (s, 2H, 1-H), 2.72 (dq, 2H, CH$_2$, ^3J = 7.8 Hz, ^4J = 1.2 Hz), 1.29 (t, 3H, CH$_3$, ^3J = 7.8 Hz). ^{13}C NMR (dichloromethane-d_2): δ 158.5 (C, C-5$_{\text{furyl}}$), 150.7 (C, C-2$_{\text{furyl}}$), 145.7 (C, C-7a), 142.6 (C, C-3a), 137.0 (C, C-2), 127.0 (CH, C-5), 124.8 (CH, C-6), 124.0 (CH, C-7), 123.9 (CH, C-3), 121.1 (CH, C-4), 108.3 (CH, C-3$_{\text{furyl}}$), 106.5 (CH, C-4$_{\text{furyl}}$), 38.4 (CH$_2$, C-1), 21.9 (CH$_2$), 12.4 (CH$_3$).

2-(5-Ethyl-2-furyl)indenyllithium (5b). Deprotonation of 2-(5-ethyl-2-furyl)indene (1.0 g, 4.75 mmol) dissolved in diethyl ether (50 mL) with *n*-butyllithium (2.9 mL, 4.75 mmol, 1.6 M in *n*-hexane) resulted in a dark red solution. After removal of the solvent the residue was suspended in pentane overnight. Filtration yielded 0.72 g (3.3 mmol, 70%) of a beige solid. ^{1}H NMR (benzene-d_6/tetrahydrofuran-d_8): δ 7.73 (m, 2H, 4-H, 7-H), 6.96 (m, 2H, 5-H, 6-H), 6.69 (s, 2H, 1-H, 3-H), 6.38 (d, 1H, 3-H$_{\text{furyl}}$, ^3J = 3.2 Hz), 5.98 (dt, 1H, 4-H$_{\text{furyl}}$, ^3J = 3.2 Hz, ^4J = 0.8 Hz), 2.58 (dq, 2H, CH$_2$, ^3J = 7.4 Hz, ^4J = 0.8 Hz), 1.16 (t, 3H, CH$_3$, ^3J = 7.4 Hz).

---

[14] Benn, R.; Grondey, H.; Nolte, R.; Erker, G. *Organometallics* **1988**, *7*, 777−778. Erker, G.; Nolte, R.; Tainturier, G.; Rheingold, A. *Organometallics* **1989**, *8*, 454−460. Erker, G.; Nolte, R.; Krüger, C.; Schlund, R.; Benn, R.; Grondey, H.; Mynott, R. *J. Organomet. Chem.* **1989**, *364*, 119−132. Benn, R.; Grondey, H.; Erker, G.; Aul, R.; Nolte, R. *Organometallics* **1990**, *9*, 2493−2497, and references therein.

[15] Erker, G.; Mühlenbernd, R.; Benn, A.; Rufiñska, A.; Tsay, Y.-H.; Krüger, C. *Angew. Chem.* **1985**, *97*, 336−337; *Angew. Chem., Int. Ed. Engl.* **1985**, *24*, 321−323. Erker, G.; Mühlenbernd, T.; Rufiñska, A.; Benn, R. *Chem. Ber.* **1987**, *120*, 507−519.

[16] Early review: Jordan, R. F. *Adv. Organomet. Chem.* **1991**, *32*, 325−387.

[17] See also: Marks, T. J. *Acc. Chem. Res.* **1992**, *25*, 57. Aulbach, M.; Küber, F. *Chem. Unserer Zeit* **1994**, *28*, 197. Bochmann, M. *J. Chem. Soc., Dalton Trans.* **1996**, 255−270, and references therein.

[18] Mallin, D. T.; Rausch, M. D.; Lin, Y.-G.; Dong, S.-H.; Chien, J. C. W. *J. Am. Chem. Soc.* **1990**, *112*, 2030. Chien, J. C. W.; Llinas, G. H.; Rausch, M. D.; Lin, Y.-G.; Winter, H. H.; Atwood, J. L.; Bott, S. G. *J. Am. Chem. Soc.* **1991**, *113*, 8569. Llinas, G. H.; Dong, S.-H.; Mallin, D. T.; Rausch, M. D.; Lin, Y.-G.; Winter, H. H.; Chien, J. C. W. *Macromolecules* **1992**, *25*, 1242. Chien, J. C. W.; Llinas, G. H.; Rausch, M. D.; Lin, Y.-G.; Winter, H. H.; Atwood, J. L.; Bott, S. G. *J. Polym. Sci., Part A* **1992**, *30*, 2601. Gauthier, W. J.; Corrigan, J. F.; Taylor, N. J.; Collins, S. *Macromolecules* **1995**, *28*, 3771−3778. Resconi, L.; Jones, R. L.; Rheingold, A. L.; Yap, G. P. A. *Organometallics* **1996**, *15*, 998−1005. Sassmannshausen, J.; Bochmann, M.; Rösch, J.; Lilge, D. *J. Organomet. Chem.* **1997**, *548*, 23−28. Averbuj, C.; Tish, E.; Eisen, M. S. *J. Am. Chem. Soc.* **1998**, *120*, 8640−8646. Bravakis, A. M.; Baily, L. E.; Pigeon, M.; Collins, S. *Macromolecules* **1998**, *31*, 1000−1009. Dietrich, U.; Hackmann, M.; Rieger, B.; Klinga, M.; Leskelä, M. *J. Am. Chem. Soc.* **1999**, *121*, 4348−4355. Kravchenko, R. L.; Sauer, B. B.; McLean, R. S.; Keating, M. Y.; Cotts, P. M.; Kim, Y. H. *Macromolecules* **2000**, *33*, 11−13. Shmulinson, M.; Galan-Fereres, M.; Lisovskii, A.; Nelkenbaum, E.; Semiat, R.; Eisen, M. S. *Organometallics* **2000**, *19*, 1208−1210.

[19] Schrock, R. R.; Fellmann, J. D. *J. Am. Chem. Soc.* **1978**, *100*, 3359−3370.

[20] Braun, S.; Kalinowski, H. O.; Berger, S. *150 and More Basic NMR Experiments;* VCH: Weinheim, 1998; and references therein.

Downloaded by CARLI CONSORTIUM on June 29, 2009
Published on October 19, 2001 on http://pubs.acs.org | doi: 10.1021/om0104518

Bis[2-(5-ethyl-2-furyl)indenyl]zirconium Dichloride (8). To a suspension of 2-(5-ethyl-2-furyl)indenyllithium (0.50 g, 2.31 mmol) in toluene was added at −78 °C solid $ZrCl_4$ (0.27 g, 1.16 mmol). The reaction mixture was allowed to warm to room temperature overnight, and the formed LiCl was filtered off. The solution was concentrated and the product was crystallized at −30 °C. The yellow crystals (0.22 g, 0.38 mmol, 35%) were suitable for an X-ray crystal structure analysis. Mp: 129 °C. Anal. Calcd for $C_{30}H_{26}Cl_2O_2Zr$ (580.7): C, 62.06; H, 5.51. Found: C, 61.79; H, 4.88. IR (KBr): $\tilde{\nu}$ 3086 (m), 3063 (w), 2972 (m), 2944 (w), 2904 (m), 1612 (w), 1561 (vs), 1437 (m), 1369 (m), 1352 (m), 1301 (m), 1210 (m), 1017 (vs), 966 (s), 842 (vs), 796 (vs), 750 (vs) cm^{-1}. ^1H NMR (dichloromethane-d_2): δ 7.27 (m, 4H, 4-H, 7-H), 7.12 (m, 4H, 5-H, 6-H), 6.57 (s, 4H, 1-H, 3-H), 6.50 (d, 2H, 3-H_{furyl}, $^3J = 3.0$ Hz), 6.19 (dt, 2H, 4-H_{furyl}, $^3J = 3.0$ Hz, $^4J = 1.2$ Hz), 2.84 (dq, 4H, CH_2, $^3J = 7.8$ Hz, $^4J = 1.2$ Hz), 1.39 (t, 6H, CH_3, $^3J = 7.8$ Hz). ^{13}C NMR (dichloromethane-d_2): δ 159.3 (C, C-5_{furyl}), 147.0 (C, C-2_{furyl}), 126.7 (CH, C-5, C-6), 125.1 (C, C-3a, C-7a), 124.9 (CH, C-4, C-7), 110.4 (CH, C-3_{furyl}), 107.1 (CH, C-4_{furyl}), 100.8 (CH, C-1, C-3), 21.9 (CH_2), 12.5 (CH_3), the resonance of C-2 could not be detected. The rotational barrier ($\Delta G^{\ddagger}_{133\ K} = 7.2 \pm 0.4$ kcal/mol) was determined by a line-shape analysis.

X-ray Crystal Structure Analysis of 8. Formula $C_{30}H_{26}O_2Cl_2Zr$, $M = 580.63$, yellow crystal 0.20 × 0.15 × 0.05 mm, $a = 23.052(1)$ Å, $b = 6.802(1)$ Å, $c = 18.587(1)$ Å, $\beta = 119.61(1)°$, $V = 2533.8(4)$ Å^3, $\rho_{calc} = 1.522$ g cm^{-3}, $\mu = 6.71$ cm^{-1}, empirical absorption correction via SORTAV ($0.877 \le T \le 0.967$), $Z = 4$, monoclinic, space group $C2/c$ (No. 15), $\lambda = 0.71073$ Å, $T = 198$ K, ω and φ scans, 4936 reflections collected ($\pm h$, $\pm k$, $\pm l$), $[(\sin \theta)/\lambda] = 0.65$ Å^{-1}, 2882 independent ($R_{int} = 0.023$) and 2565 observed reflections [$I \ge 2\sigma(I)$], 160 refined parameters, $R = 0.026$, $wR_2 = 0.063$, max. residual electron density 0.28 (−0.33) e Å^{-3}, hydrogens calculated and refined as riding atoms.[21]

Bis[2-(5-methyl-2-furyl)indenyl]zirconium Dichloride (6a). ^1H NMR ($CDFCl_2$, CDF_2Cl, 253 K): δ 7.24 (m, 4H, 4-H, 7-H), 7.10 (m, 4H, 5-H, 6-H), 6.64 (s, 4H, 1-H, 3-H), 6.45 (d, 2H, 3-H_{furyl}, $^3J = 3.6$ Hz), 6.14 (dq, 2H, 4-H_{furyl}, $^3J = 3.6$ Hz, $^4J = 1.2$ Hz), 2.48 (s, 6H, CH_3). ^1H NMR ($CDFCl_2$, CDF_2Cl, 133 K): δ 7.30−6.14 (m, arom. CH), 2.57 (s, CH_3), 2.44 (s, CH_3*). The rotational barrier ($\Delta G^{\ddagger}_{133\ K} = 7.0 \pm 0.3$ kcal/mol) was determined by a line-shape analysis.

Bis[2-(5-methyl-2-thienyl)indenyl]zirconium Dichloride (9a). ^1H NMR ($CDFCl_2$, CDF_2Cl, 253 K): δ 7.21 (m, 4H, 4-H, 7-H), 7.12 (m, 4H, 5-H, 6-H), 7.01 (d, 2H, 3-$H_{thienyl}$, $^3J = 3.6$ Hz), 6.79 (dq, 2H, 4-$H_{thienyl}$, $^3J = 3.6$ Hz, $^4J = 0.6$ Hz), 6.60 (s, 4H, 1-H, 3-H), 2.58 (d, 6H, CH_3, $^4J = 0.6$ Hz). ^1H NMR ($CDFCl_2$, CDF_2Cl, 133 K): δ 7.24−6.65 (m, arom. CH), 2.60 (s, CH_3), 2.57 (s, CH_3*). The rotational barrier ($\Delta G^{\ddagger}_{133\ K} = 6.7 \pm 0.3$ kcal/mol) was determined by a line-shape analysis.

Bis[2-(5-methyl-2-furyl)indenyl]zirconium Dibromide (6b). To a stirred suspension of 2-(5-methyl-2-furyl)indenyllithium (**5a**) (0.50 g, 2.47 mmol) in 50 mL of toluene was added at −78 °C a suspension of $ZrBr_4$ (0.51 g, 1.24 mmol) in toluene. The resultant reaction mixture was allowed to warm to room temperature and then filtered to separate the LiBr. Crystallization at −30 °C yielded 0.29 g (0.45 mmol, 37%) of an orange solid. Mp: 161 °C. Anal. Calcd for $C_{28}H_{22}Br_2O_2Zr$ (641.5): C, 52.42; H, 3.46. Found: C, 52.01; H, 3.57. IR (KBr): $\tilde{\nu}$ 3130 (w), 3013 (w), 2944 (w), 1619 (w), 1566 (vs), 1529 (m), 1433 (m), 1343 (m), 1200 (s), 1025 (s), 977 (m), 951 (m), 861 (s), 829 (s), 802 (vs), 744 (vs) cm^{-1}. ^1H NMR (dichloromethane-d_2): δ 7.28 (m, 4H, 4-H, 7-H), 7.12 (m, 4H, 5-H, 6-H), 6.68 (s, 4H, 1-H, 3-H), 6.49 (dd, 2H, 3-H_{furyl}, $^3J = 1.8$ Hz, $^5J = 0.6$ Hz), 6.17 (dq, 2H, 4-H_{furyl}, $^3J = 1.8$ Hz, $^4J = 1.2$ Hz), 2.48 (dd, 6H, CH_3, $^4J = 1.2$ Hz, $^5J = 0.6$ Hz). ^{13}C NMR (dichloromethane-d_2): δ 153.7 (C, C-5_{furyl}), 147.3 (C, C-2_{furyl}), 126.9 (CH, C-5, C-6), 126.5 (C, C-3a, C-7a), 125.5 (CH, C-4, C-7), 124.7 (C, C-2), 110.9 (CH, C-3_{furyl}), 108.8 (CH, C-4_{furyl}), 101.2 (CH, C-1, C-3), 14.0 (CH_3). The rotational barrier ($\Delta G^{\ddagger}_{133\ K} = 7.2 \pm 0.3$ kcal/mol) was determined by a line-shape analysis.

Bis[2-(5-methyl-2-thienyl)indenyl]zirconium Dibromide (9b). Analogously as described above, 2-(5-methyl-2-thienyl)indenyllithium (**5c**) (0.50 g, 2.29 mmol) was reacted with $ZrBr_4$ (0.47 g, 1.14 mmol) to yield 0.14 g (0.21 mmol, 19%) of an orange-brown product. Mp: 133 °C. Anal. Calcd for $C_{28}H_{22}Br_2O_2Zr$ (641.5): C, 49.92; H, 3.92. Found: C, 50.37; H, 3.77. IR (KBr): $\tilde{\nu}$ 3114 (w), 3058 (w), 2927 (w), 2858 (w), 1618 (w), 1539 (w), 1510 (s), 1448 (m), 1380 (w), 1340 (w), 1227 (w), 1057 (w), 842 (vs), 819 (vs), 813 (vs), 751 (vs) cm^{-1}. ^1H NMR (dichloromethane-d_2): δ 7.22 (m, 4H, 4-H, 7-H), 7.12 (m, 4H, 5-H, 6-H), 7.05 (d, 2H, 3-$H_{thienyl}$, $^3J = 3.6$ Hz), 6.80 (dq, 2H, 4-$H_{thienyl}$, $^3J = 3.6$ Hz, $^4J = 1.2$ Hz), 6.60 (s, 4H, 1-H, 3-H), 2.58 (d, 6H, CH_3, $^4J = 1.2$ Hz). ^{13}C NMR (dichloromethane-d_2): δ 142.3 (C, C-$5_{thienyl}$), 134.8 (C, C-$2_{thienyl}$), 128.3 (C, C-2), 127.1 (CH, C-5, C-6), 126.9 (CH, C-$3_{thienyl}$), 126.8 (CH, C-4 $_{thienyl}$), 126.5 (C, C-3a, C-7a), 125.5 (CH, C-4, C-7), 103.6 (CH, C-1, C-3), 15.7 (CH_3). The rotational barrier ($\Delta G^{\ddagger}_{133\ K} = 6.9 \pm 0.3$ kcal/mol) was determined by a line-shape analysis.

Bis[2-(5-methyl-2-furyl)indenyl]dineopentylzirconium (7b). Bis[2-(5-methyl-2-furyl)indenyl]zirconium dichloride (**6a**) (0.4 g, 0.72 mmol) was suspended in diethyl ether (40 mL) and at −78 °C was added a solution of neopentyllithium (11.0 mL, 2.88 mmol, 0.26 M in isohexane). After stirring overnight the solvent was removed in vacuo and pentane was added. The formed LiCl was filtered off and the product was crystallized at −30 °C. A second crystallization yielded 0.27 g (0.43 mmol, 60%) of an off-white solid. Mp: 142 °C (decomp). HRMS: $C_{29}H_{25}O_2Zr$ ($M^+ - CH_2C(CH_3)_3$; $-CH_2{=}C(CH_3)_2$), requires 495.09015, found m/z 495.08805. IR (KBr): $\tilde{\nu}$ 3131 (w), 3058 (w), 2950 (vs), 2893 (s), 2870 (m), 1573 (s), 1448 (m), 1363 (s), 1233 (m), 1204 (m), 1097 (m), 1023 (vs), 944 (m), 836 (vs), 791 (vs), 745 (vs) cm^{-1}. ^1H NMR (dichloromethane-d_2): δ 6.98 (m, 4H, 4-H, 7-H), 6.85 (m, 4H, 5-H, 6-H), 6.67 (s, 4H, 1-H, 3-H), 6.47 (dd, 2H, 3-H_{furyl}, $^3J = 3.6$ Hz, $^5J = 0.6$ Hz), 6.20 (dq, 2H, 4-H_{furyl}, $^3J = 3.6$ Hz, $^4J = 1.2$ Hz), 2.47 (d, 6H, CH_3, $^4J = 1.2$ Hz), 0.83 (s, 18H, $C(CH_3)_3$), −1.25 (s, 4H, CH_2). ^{13}C NMR (dichloromethane-d_2): δ 152.3 (C, C-5_{furyl}), 148.4 (C, C-2_{furyl}), 125.4 (C, C-3a, C-7a), 125.1 (CH, C-4, C-7), 124.3 (CH, C-5, C-6), 119.3 (C, C-2), 108.5 (CH, C-3_{furyl}), 108.2 (CH, C-4_{furyl}), 95.2 (CH, C-1, C-3), 84.8 (CH_2), 36.8 ($C(CH_3)_3$), 34.7 ($C(CH_3)_3$), 13.9 (CH_3). The rotational barriers ($\Delta G^{\ddagger}_{rot(Cp)} = 9.0 \pm 0.3$ kcal/mol, $\Delta G^{\ddagger}_{rot(Ar)} = 7.1 \pm 0.4$ kcal/mol) were determined by a line-shape analysis.

X-ray Crystal Structure Analysis of 7b. Formula $C_{38}H_{44}O_2Zr$, $M = 623.95$, yellow crystal 0.50 × 0.40 × 0.35 mm, $a = 10.829(1)$ Å, $b = 17.669(1)$ Å, $c = 17.130(1)$ Å, $\beta = 101.12(1)°$, $V = 3216.1(4)$ Å^3, $\rho_{calc} = 1.289$ g cm^{-3}, $\mu = 3.73$ cm^{-1}, empirical absorption correction via SORTAV ($0.835 \le T \le 0.881$), $Z = 4$, monoclinic, space group $C2/c$ (No. 15), $\lambda = 0.71073$ Å, $T = 198$ K, ω and φ scans, 9821 reflections collected ($\pm h$, $\pm k$, $\pm l$), $[(\sin \theta)/\lambda] = 0.65$ Å^{-1}, 3638 independent ($R_{int} = 0.029$) and 3290 observed reflections [$I \ge 2\sigma(I)$], 221 refined parameters, $R = 0.038$, $wR_2 = 0.088$, max. residual electron density 0.62 (−0.55) e Å^{-3}, disorder in the *tert*-butyl group, refined with split positions and geometrical restraints, hydrogens calculated and refined as riding atoms.[21]

Dibenzylbis[2-(5-methyl-2-furyl)indenyl]zirconium (7c). Bis[2-(5-methyl-2-furyl)indenyl]zirconium dichloride (**6a**) (0.50 g, 0.91 mmol) was suspended in diethyl ether/tetrahydrofuran (40 mL/20 mL), and a solution of benzylmagnesium chloride (1.81 mL, 1.81 mmol, 1.00 M solution in diethyl ether) was added. The suspension was stirred for 6 h at room tempera-

---

(21) Data sets were collected with a Nonius KappaCCD diffractometer, equipped with a rotating anode generator Nonius FR591. Programs used: data collection COLLECT (Nonius B.V., 1998), data reduction Denzo-SMN (Z. Otwinowski, W. Minor, *Methods Enzymol.* **1997**, *276*, 307−326), absorption correction SORTAV (R. H. Blessing, *Acta Crystallogr.* **1995**, *A51*, 33−37; R. H. Blessing, *J. Appl. Crystallogr.* **1997**, *30*, 421−426), structure solution SHELXS-97 (G. M. Sheldrick, *Acta Crystallogr.* **1990**, *A46*, 467−473), structure refinement SHELXL-97 (G. M. Sheldrick, Universität Göttingen, 1997), graphics DIAMOND (K. Brandenburg, Universität Bonn, 1997).

ture, and the solvent was removed in vacuo. Toluene (50 mL) was added and then the reaction mixture was filtered. Crystallization at −30 °C, filtration, and washing with toluene (10 mL) and pentane yielded 0.20 g (0.30 mmol, 33%) of a yellow solid. Mp: 65 °C. HRMS: $C_{35}H_{29}O_2Zr$ ($M^+ - CH_2Ph$), requires 571.12146, found *m*/*z* 571.12288. IR (KBr): $\tilde{\nu}$ 3120 (w), 3075 (w), 3023 (w), 2916 (w), 1595 (s), 1573 (s), 1488 (s), 1437 (m), 1374 (m), 1210 (vs), 1029 (s), 995 (vs), 965 (m), 859 (vs), 785 (s), 757 (vs), 706 (s) cm^{-1}. ^1H NMR (dichloromethane-d_2): δ 7.20 (t, 4H, *m*-H, $^3J = 8.4$ Hz, $^3J = 7.2$ Hz), 7.05 (m, 4H, 4-H, 7-H), 6.68 (t, 2H, *p*-H, $^3J = 7.2$ Hz), 6.73 (d, 4H, *o*-H, $^3J = 8.4$ Hz), 6.69 (m, 4H, 5-H, 6-H), 6.45 (d, 2H, 3-H_{furyl}, $^3J = 3.0$ Hz), 6.24 (dq, 2H, 4-H_{furyl}, $^3J = 3.0$ Hz, $^4J = 1.2$ Hz), 6.05 (s, 4H, 1-H, 3-H), 2.55 (d, 6H, CH_3, $^3J = 1.2$ Hz), 0.14 (bs, 4H, CH_2). ^{13}C NMR (dichloromethane-d_2): δ 153.6 (C, *ipso*-C), 152.9 (C, C-5_{furyl}), 147.7 (C, C-2_{furyl}), 128.2 (CH, *m*-C), 126.1 (CH, *o*-C), 125.9 (CH, C-4, C-7), 125.4 (C, C-3a, C-7a), 124.7 (CH, C-5, C-6), 121.3 (CH, *p*-C), 121.2 (C, C-2), 108.9 (CH, C-3_{furyl}), 108.5 (CH, C-4_{furyl}), 66.9 (CH_2), 13.9 (CH_3). C-1, C-3 was not detected. The rotational barriers ($\Delta G^{\ddagger}_{rot(Cp)} = 11.4 \pm 0.3$ kcal/mol, $\Delta G^{\ddagger}_{rot(Ar)} = 7.3 \pm 0.4$ kcal/mol) were determined by a line-shape analysis.

Dibenzylbis[2-(5-methyl-2-thienyl)indenyl]zirconium (10b). Analogously as described above, bis[2-(5-methyl-2-thienyl)indenyl]zirconium dichloride (**9a**) (0.50 g, 0.86 mmol) was reacted with a solution of benzylmagnesium chloride (1.72 mL, 1.72 mmol, 1.00 M in diethyl ether) to yield 0.34 g (0.48 mmol, 57%) of the yellow product. Mp: 107 °C. HRMS: $C_{35}H_{29}S_290_{Zr}$ ($M^+ - CH_2Ph$), requires 603.07581, found *m*/*z* 603.07424. IR (KBr): $\tilde{\nu}$ 3052 (w), 3012 (m), 2916 (w), 1601 (s), 1488 (s), 1448 (m), 1369 (m), 1211 (m), 1017 (m), 989 (s), 881 (m), 836 (vs), 808 (s), 751 (vs), 700 (vs) cm^{-1}. ^1H NMR (dichloromethane-d_2): δ 7.21 (t, 4H, *m*-H, $^3J = 7.8$ Hz, $^3J = 6.6$ Hz), 7.05 (m, 4H, 4-H, 7-H), 6.99 (d, 2H, 3-$H_{thienyl}$, $^3J = 3.6$ Hz), 6.88−6.86 (m, 4H, *p*-H, 4-$H_{thienyl}$), 6.79 (d, 4H, *o*-H, $^3J = 6.6$ Hz), 6.68 (m, 4H, 5-H, 6-H), 5.87 (bs, 4H, 1-H, 3-H), 2.63 (d, 6H, CH_3, $^4J = 1.2$ Hz), 0.24 (bs, 4H, CH_2). ^{13}C NMR (dichloromethane-d_2): δ 153.0 (C, *ipso*-C), 140.9 (C, C-$5_{thienyl}$), 136.0 (C, C-$2_{thienyl}$), 128.3 (CH, *m*-C), 126.7 (CH, C-$4_{thienyl}$), 126.4 (CH, *o*-C), 126.0, (CH, C-4, C-7), 125.9 (C, C-3a, C-7a), 125.5 (C, C-2), 125.0 (CH, C-5, C-6), 124.8 (CH, C-$3_{thienyl}$), 121.5 (CH, *p*-C), 66.4 (CH_2), 15.7 (CH_3). C-1, C-3 was not detected. The rotational barrier ($\Delta G^{\ddagger}_{rot(Cp)} = 12.0 \pm 0.3$ kcal/mol) was determined by a line-shape analysis.

Acknowledgment. Financial support from the Fonds der Chemischen Industrie and the Deutsche Forschungsgemeinschaft is gratefully acknowledged. E.W. thanks the Academy of Finland for financial support.

Supporting Information Available: Detailed information about the X-ray crystal structure analyses of the complexes **7b** and **8**, series of the dynamic ^1H NMR spectra, and the line-shape analysis of the compounds **6a**, **6b**, **6c**, **7b**, **7c**, **9a**, **9b**, and **10b**. This material is available free of charge via the Internet at http://pubs.acs.org.

OM0104518

Downloaded by CARLI CONSORTIUM on June 29, 2009
Published on October 19, 2001 on http://pubs.acs.org | doi: 10.1021/om0104518